Spin-dependent electronic band structure of Co/Cu(001) with different film thicknesses

2008 J. Phys.: Condens. Matter 20 225001

(http://iopscience.iop.org/0953-8984/20/22/225001)

J. Phys.: Condens. Matter **20** (2008) 225001 (5pp) doi:10.1088/0953-8984/20/22/225001

Spin-dependent electronic band structure of Co/Cu(001) with different film thicknesses

K Miyamoto[1], K Iori[1], K Sakamoto[1], A Kimura[1], S Qiao[2], K Shimada[2], H Namatame[2] and M Taniguchi[1,2]

[1] Graduate School of Science, Hiroshima University, 1-3-1 Kagamiyama, Higashi-Hiroshima 739-8526, Japan
[2] Hiroshima Synchrotron Radiation Center, Hiroshima University, 2-313 Kagamiyama, Higashi-Hiroshima 739-0046, Japan

E-mail: kmiyamoto@hiroshima-u.ac.jp

Received 29 November 2007, in final form 5 March 2008
Published 16 April 2008
Online at stacks.iop.org/JPhysCM/20/225001

Abstract
Spin- and angle-resolved photoemission spectroscopy (SARPES) has been applied to the study of spin-polarized electronic structures of face-centered tetragonal (fct) Co thin films with thicknesses from 2 to 9.5 monolayers (MLs). We have clearly observed two dispersive majority and minority spin band structures originating from the bulk-like bands. These observed band structures show narrower width for thinner film due to an in-plane lattice expansion at the Co–Cu interface.

(Some figures in this article are in colour only in the electronic version)

1. Introduction

Magnetic thin films are expected to show peculiar magnetic properties such as an enhanced magnetic moment, a strong magnetic anisotropy, and a reduced Curie temperature, which are generally very different from those of bulk [1–3]. The metallic synthetic lattice, which is a nanoscale magnetic material grown on a semiconductor or a metallic surface, has lately attracted considerable attention. In metallic thin films, the difference in the lattice constant of the substrate results in variations of the structure and magnetic properties. It is known that bulk Co has a hexagonal close-packed (hcp) structure at room temperature. In contrast, Co growing in the fcc lattice shows a small tetragonal distortion (∼4%) along the surface normal [4]. As for magnetic properties, Co/Cu(001) shows an in-plane magnetic anisotropy along the [1$\bar{1}$0] direction and the Curie temperature already exceeds room temperature at 2 ML [5]. Enhanced spin and orbital magnetic moments for thinner films of Co/Cu(001) have been experimentally clarified by the x-ray magnetic circular dichroism technique [6]. Such an enhancement could be pertinent to a reduced dimensionality, which might cause a large exchange splitting and/or a strong electron localization. The enhancement of 3d exchange splitting was suggested for 2.4 ML Co/Cu(001) by spin-resolved photoelectron spectroscopy (PES) at $\bar{\Gamma}$, where the energy dispersion feature was missing [7]. The Co/Cu superlattice is well known to show an oscillatory magnetic interlayer coupling [8] as well as a giant magneto-resistance (GMR) at room temperature [9]. Such striking magnetic and transport properties are determined by spin-dependent electronic structure at the Co–Cu interface. It is expected that a knowledge of momentum- and spin-dependent electronic structures of face-centered tetragonal (fct) Co/Cu(001) in the vicinity of the Fermi level (E_F) would help us to understand the behavior of spin-polarized electron current in multilayer systems. Motivated by these aspects, we have tried to clarify how the Co 3d states depend on the film thickness (>2 ML) by spin- and angle-resolved photoelectron spectroscopy (SARPES) in the wide range of the Brillouin zone.

2. Experimental details

A clean surface of Cu substrate was obtained by repeated cycles of Ar-ion bombardment (1–2 keV) and annealing at 720 K under ultra high vacuum conditions. Co thin film was epitaxially grown by a commercial evaporator at

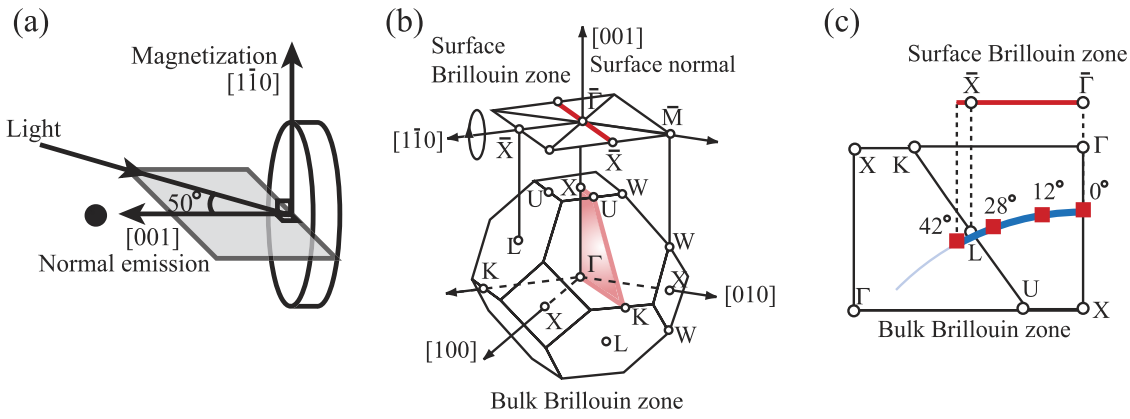

Figure 1. (a) Experimental setup for SARPES measurements of fct Co/Cu(001). (b) Surface and bulk Brillouin zones for (001) surface of fcc lattice. Here, the thick line along $\bar{\Gamma}$–$\bar{X}$ in the surface Brillouin zone and the shaded area in the bulk Brillouin zone show observed direction and area in the present experiment. (c) Cross section of the bulk Brillouin zone at the ΓXUK plane. The thick line and square symbol correspond to the measured wavenumbers at E_F in this experiment.

a deposition rate of 0.1–0.2 ML min^{-1} in a pressure of 5×10^{-8} Pa. The substrate was kept at room temperature during the Co film growth. The cleanliness and flatness of the substrate and film surfaces were checked by means of Auger electron spectroscopy (AES) and reflection high energy electron diffraction (RHEED). The Co film thickness was estimated from RHEED as well as the intensity ratio of the Co first *LMM* signal ($E_k = 670$ eV) to that of the Cu third *LMM* ($E_k = 940$ eV) in the AES spectrum. The SARPES was performed using our home-made system equipped with a 125 mm radius hemispherical electron analyzer (Omicron:EA-125) and the retarding type Mott spin polarimeter at the Hiroshima Synchrotron Radiation Center, which was originally designed by Qiao *et al* [10]. Moreover, we have evaluated the efficiency of the spin polarimeter by finding the effective Sherman function and the intensity of scattered electrons with our recently developed self-calibration method [11]. All of the spectra were measured at room temperature ($T \sim 300$ K) and excited by an unpolarized He I_α resonance line ($h\nu \sim 21.2$ eV). Angular acceptance of photoelectrons was set to 2° at a pass energy of 5 eV. The energy resolution is 110 meV with these experimental conditions, as checked by the spectrum of polycrystalline gold close to E_F. The geometry of the measurement is shown in figure 1(a). The sample was magnetized along the in-plane [1$\bar{1}$0] direction by a coil wound around a μ-metal yoke. The measured spin component for the present experiment is aligned along the magnetization direction. The angle of incident light was 50° relative to the surface normal. In figure 1(b), the thick line represents the $\bar{\Gamma}$–$\bar{X}$ line in the surface Brillouin zone and the shaded area denotes the ΓXUK plane in the bulk Brillouin zone, traced in the present experiment. A free electron final state assumes parallel and perpendicular wavenumber components of the electronic state at E_F as $k_\parallel = 0.512\sqrt{h\nu - E_B - \phi}\sin\theta$ and $k_\perp = 0.512\sqrt{(h\nu - E_B - \phi)\cos^2\theta + V_0}$, respectively, as denoted by the thick curve in figure 1 (c), where $h\nu$, E_B, ϕ, and V_0 represent photon energy, binding energy, work function, and inner potential. Here, the inner potential V_0 of 15 eV has been referred to the previous report [13]. The spectra were recorded by repeated scans and the direction of magnetization was reversed for every new scan to cancel out the instrumental asymmetry. The magnetization reversal also minimizes the contribution of spin–orbit induced spin polarization compared to that induced by the exchange-interaction, which is of interest in this work [13, 14].

3. Results and discussion

Figures 2(a) and (b) show the SARPES spectra and the spin polarizations of 9.5 ML Co/Cu (001) at emission angles (θ) of 0°–42°. Here, majority and minority spin spectra are shown with open and filled triangles, respectively. Thick (thin) vertical bars show the peak positions of Co 3d states in the majority (minority) spin channel. At $\theta = 0°$, the minority spin spectrum possesses a peak at a binding energy (E_B) of 0.21 (±0.09) eV as denoted by A in figure 2(a). The peak A shifts toward higher E_B with increasing θ and reaches an E_B maximum at around $\theta = 37°$ ($\bar{X}$ point). In contrast, a broad peak (named B) is found for the majority spin spectrum at $E_B = 0.8$ (±0.12) eV, showing energy shift toward lower E_B with increasing θ and it reaches near Fermi level (E_F) at $\theta = 12°$. In the normal emission spectrum, the observed features of majority and minority spin spectra are in principle consistent with the reported result with a different photon energy of $h\nu = 24$ eV [12]. Here, we have found the largest negative spin polarization of −50% near E_F and a positive value of 30% in the E_B region of 1.5–2.0 eV without exhibiting any distinct structures. The minimum of negative spin polarization moves to higher E_B with increasing θ and reaches an E_B maximum at around $\theta = 37°$. It is noticed that a finite spin polarization of 30% found above E_F is derived from spin-polarized secondary electrons excited by both He I_β ($h\nu = 23.1$ eV) and He II_α ($h\nu = 40.8$ eV) lines. Since the background intensities produced by He I_β and He II_α are very poor, it should not influence the following discussion in this paper.

Next, the experimentally determined energy dispersion curves are presented in figure 3. It is found here that the

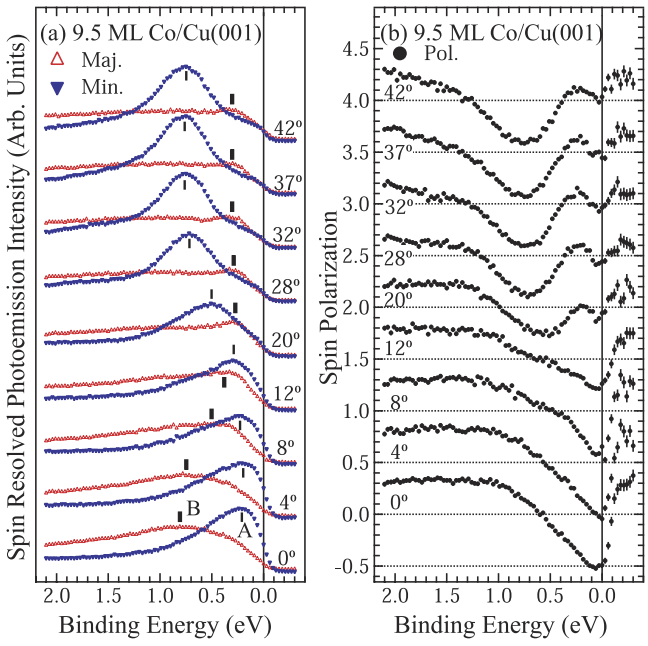

Figure 2. (a) SARPES spectra and (b) spin polarizations of 9.5 ML Co/Cu(001) with emission angles from 0° to 42°. Majority and minority spin spectra are shown with open and filled triangles, respectively. Thin (thick) vertical bars show the peak positions of Co 3d states in the minority (majority) spin channel. Origins of spin polarizations are shifted by 0.5 for every emission angle.

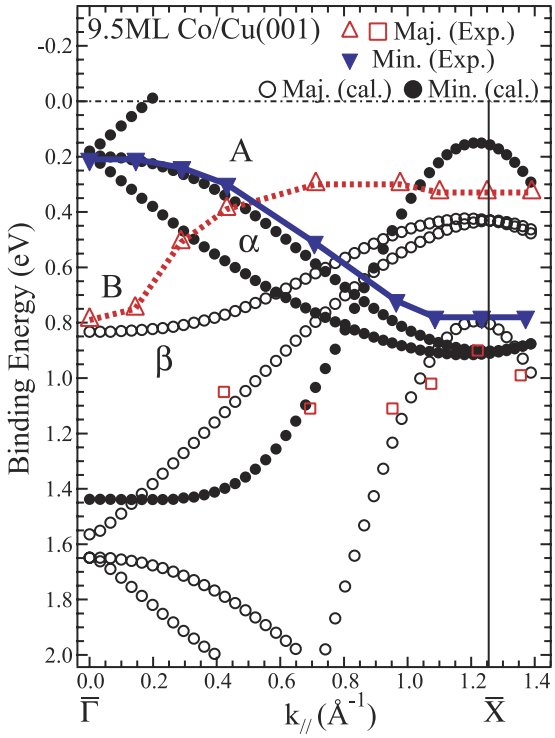

Figure 3. Experimental E_B-$k_\parallel$ plots for majority and minority spin states as denoted by open and filled triangles, respectively. Solid and dashed lines show the interpolated band dispersions of bands A and B. Calculated bulk band structures obtained by the tight-binding scheme are superposed with open and filled circles for majority and minority spin states, respectively.

experimental minority spin band A shows a downward energy dispersion along $\bar{\Gamma}$–$\bar{X}$, as shown with filled triangles, while the majority spin band B shows an upward dispersion, as denoted by open triangles. The other weak emission features are also plotted with open squares. It is recognized that the bottom of the energy dispersion curve of minority spin band (B) is located at the $\bar{X}$ point in the surface Brillouin zone (SBZ). Here, the energy dispersions of A and B are compared with the calculations obtained by a tight-binding method along the thick curve shown in figure 1(c). In the calculation, only the first and second nearest neighbor atoms are considered. The transfer integrals such as (spσ) and (pdσ) etc have been determined by fitting to the reported pseudopotential calculation [15]. Here, the parameter of exchange splitting energy was set to 1.5 eV, which is the same as that reported by Fanelsa *et al* [13]. Open (filled) circles represent the calculated band structure for majority (minority) spin states. The experimental energy dispersion curves are interpolated between the experimental data points for A and B. It is recognized that one of the calculated minority spin bands (α: filled circles) also shows downward dispersion that reaches the bottom at point $\bar{X}$, which is similar to the experimental result for A. The observed bandwidth and the dispersion feature are similar to the calculated ones, as shown in figure 3. Besides, the experimental majority spin band B corresponds to the calculated band (β: open circles). Accordingly, these observed band structures (A and B) can be regarded as those from bulk. At $\bar{\Gamma}$, minority and majority spin structures A and B can be assigned to $\Delta_{5\downarrow}$ and $\Delta_{2\uparrow}$ states, respectively. It is noted that only the states with Δ_1 and Δ_5 orbital symmetries can be accessible for the excitation with s- and p-polarized light. However, there is a possibility that the Δ_2 state can be observed due to an inter-band mixing of Δ_2 and Δ_5 bands through a spin–orbit coupling, as shown in the similar argument for Cu(001) [16].

Figures 4(a)–(d) show the observed SARPES spectra of the Co films with different thicknesses (2–9.5 ML) for majority and minority spin states at $\bar{\Gamma}$ and $\bar{X}$ points. Here, we mainly discuss the band structures A and B in the minority and majority spin channels. At first, in the majority spin state of figure 4(a), we find that the energy position of structure B shifts toward higher E_B with increasing film thickness at point $\bar{\Gamma}$. The energy difference of the spectra for 2 and 9.5 ML is about 400 meV. In the minority spin channel of figure 4(b) at point $\bar{\Gamma}$, the peak A is located at lower E_B for thicker film and the maximum energy difference is as large as about 100 meV. In contrast, at point $\bar{X}$, the energy position for the peak B (A) in the majority (minority) spin channel shifts toward lower (higher) E_B with increasing film thickness. The largest energy shift of band B (A) is about 60 meV (270 meV). Thus, the observed energy shifts are dependent on the electronic states (A or B) as well as on the symmetry point of the SBZ.

Figures 5(a) and (b) are shown to clarify these experimental band dispersion curves of films with different thicknesses (2–9.5 ML) for the majority and minority spin states. As described in the previous paragraph, the energy position of A shifts toward lower E_B with increasing film

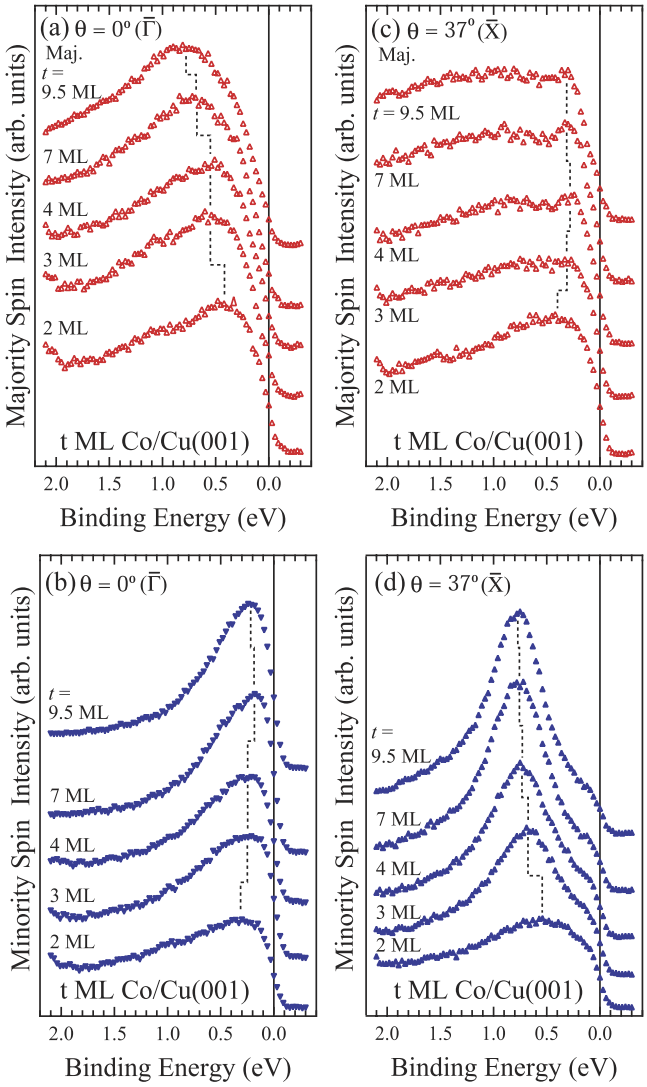

Figure 4. Majority (minority) spin spectra of t ML Co/Cu(001) with $t = 2$, 3, 4, 7, and 9.5 ML for $\theta = 0°$ ((a), (b)) and for $\theta = 37°$ ((c), (d)), corresponding to $\bar{\Gamma}$ and $\bar{X}$ points of the surface Brillouin zone, respectively.

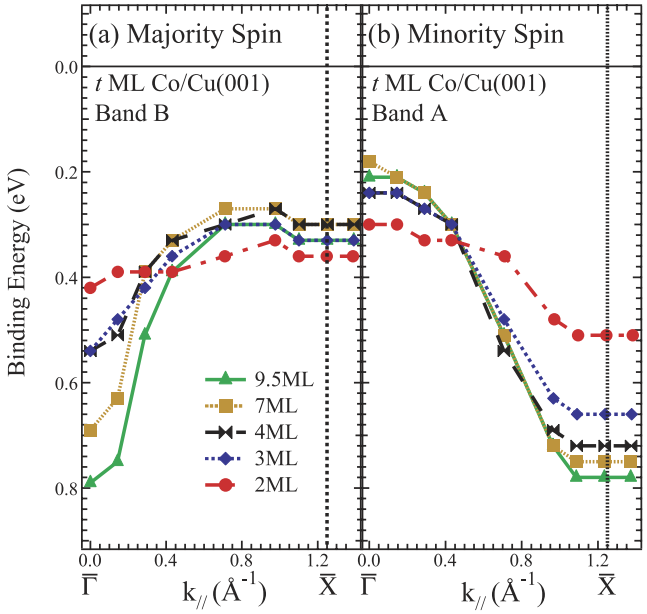

Figure 5. (a), (b) Experimental band dispersion curves for t ML Co/Cu(001) with $t = 2$, 3, 4, 7, and 9.5 ML for bands B (left) and A (right).

thickness at point $\bar{\Gamma}$, while the behavior is opposite at point $\bar{X}$. As a result, the bandwidth defined as the difference of peak positions between $\bar{\Gamma}$ and $\bar{X}$ of A appears to be narrower from 570 to 210 meV with decreasing the film thickness from 9.5 to 2 ML. As for the majority spin band B, the width is also narrowed from 460 to 60 meV when the film thickness decreases, as shown in figure 4(a). In particular, the majority spin band B of 2 ML Co film seems to have negligible dispersion, while the minority spin band A for 2 ML Co film still appears to retain its dispersion. The thicker films above 7 ML show a similar bandwidth for A, while for B, the width is still reduced by 100 meV. As reported in the previous paper by Schneider *et al*, the electronic structure of 5 ML fct-cobalt film is considered to be already bulk-like [12]. This is supported by the present result for band A corresponding to the same symmetry (Δ_5 at $\bar{\Gamma}$). On the other hand, for band B with different symmetry (Δ_2 at $\bar{\Gamma}$), the width is even different between 7 and 9.5 ML. This result means that band structures with different spatial symmetry are affected by the film thickness in a different way. Moreover, the size of peak shift related to film thickness depends on the position of $k_\parallel$ such as $\bar{\Gamma}$ and $\bar{X}$, as shown in figure 4. According to the present analysis with tight-binding calculation, band A is composed of only the d_{xz} (d_{yz}) orbital at $\bar{\Gamma}$ and a linear combination of $d_{x^2-y^2}$ (∼62%), d_{xz} (∼18%), and d_{yz} (∼18%) at $\bar{X}$, where x-, y-, and z-axes are defined along [100], [010], and [001] of figure 1(b). Similarly, for band B, it is only derived from the $d_{x^2-y^2}$ orbital at $\bar{\Gamma}$ and composed of a linear combination of $d_{x^2-y^2}$ (∼37%), d_{xz} (∼31%), d_{yz} (∼31%) orbitals at $\bar{X}$. It is noted that the distinct energy shift emerges for the specific states dominated by the $d_{x^2-y^2}$ orbital. It is considered that the narrower bandwidth with decreasing film thickness indicates a less delocalized feature of Co 3d electrons. If the electron localization is derived from a low dimensionality, the bandwidth would be narrow especially along the normal direction to the surface plane. Since the emission angle is varied with fixed photon energy in the present experiment, the band structures are traced not only along $k_\parallel$ but also along $k_\perp$. One would expect the band narrowing along $k_\perp$ direction because the electron motion could be limited to the plane. However, this interpretation is incompatible with the observed narrowing of the $d_{x^2-y^2}$ band that is spread along the surface plane. Here, the transfer integrals for the tight-binding calculation which are sensitively dependent on the Co–Co distance, are responsible for the bandwidth. Generally, the bandwidth is narrower since the transfer integral becomes smaller when the Co–Co distance increases. Therefore, it is suggested that the Co–Co distance of the thin film is more expanded along the in-plane direction for thinner film thickness, because the atomic distance of Cu is generally larger than that of Co [17, 18]. Besides, it is also necessary to consider the atomic inter-diffusion effect at the interface between Co and Cu layers instead of the electron localization

due to a lower dimensionality. Actually, it is known that the in-plane lattice constant could be expanded, as caused by atomic inter-diffusion, because the surface energy of fcc Cu(001) is about half as small as that of fcc Co(001) [19, 20]. Therefore, it is concluded that the observed feature of the band structure for thinner film thickness is mainly derived from the expanded lattice constant of the Co film caused by the inter-diffusion effect or by the Cu substrate itself.

4. Conclusion

In conclusion, we have performed spin- and angle-resolved photoemission spectroscopy to investigate variation of the spin-polarized electronic states for fct Co with changing film thickness. It has been found that the majority and minority spin band dispersions become flatter as the Co film thickness decreases, indicating less hopping probability of the Co 3d electrons in the thinner film, which is not caused simply by the lower dimensionality but more seriously by the increase of the lateral lattice constant.

References

[1] O'Brien W L, Droubay T and Tonner B P 1996 *Phys. Rev.* B **54** 9297
[2] Matsumura D, Yokoyama T, Amamiya K, Kitagawa S and Ohta T 2002 *Phys. Rev.* B **66** 024402
[3] Gambardella P, Dallmeyer A, Maiti K, Malagoli M C, Eberhardt W, Kern K and Carbone C 2002 *Nature* **416** 301
[4] Schneider C M, Schuster P, Hammond M, Ebert H, Noffke J and Kirschner J 1991 *J. Phys.: Condens. Matter* **3** 4349
[5] Huang F, Kief M T, Mankey G J and Willis R F 1994 *Phys. Rev.* B **49** 3962
[6] Tischer M, Hjortstam O, Arvanitis D, Hunter Dunn J, May F, Baberschke K, Trygg J, Wills J M, Johansson B and Eriksson O 1995 *Phys. Rev. Lett.* **75** 1602
[7] Clemens W, Vescovo E, Kachel T, Carbone C and Eberhardt W 1992 *Phys. Rev.* B **46** 4198
Clemens W, Kachel T, Rader O, Vescovo E, Blügel S, Carbone C and Eberhardt W 1992 *Solid State Commun.* **81** 739
[8] Parkin S S P, Bhadra R and Roche K P 1991 *Phys. Rev. Lett.* **66** 2152
[9] Baibich M N, Broto J M, Fert A, Nguyen Van Dau F, Petroff F, Eitenne P, Creuzet G, Friederich A and Chazelas J 1988 *Phys. Rev. Lett.* **61** 2472
[10] Qiao S, Kimura A, Harasawa A, Sawada M, Chung J G and Kakizaki A 1997 *Rev. Sci. Instrum.* **68** 4390
[11] Iori K, Miyamoto K, Narita H, Sakamoto K, Kimura A, Qiao S, Shimada K, Namatame H and Taniguchi M 2006 *Rev. Sci. Instrum.* **77** 013101
[12] Schneider C M, de Miguel J J, Bressler P, Schuster P, Miranda R and Kirschner J 1990 *J. Electron Spectrosc. Relat. Phenom.* **51** 263
[13] Fanelsa A, Kisker E, Henk J and Feder R 1996 *Phys. Rev.* B **54** 2922
[14] Henk J, Scheunemann T, Halilov S V and Feder R 1996 *J. Phys.: Condens. Matter* **8** 47
[15] Himpsel F J, Ortega J E, Mankey G M and Willis R F 1998 *Adv. Phys.* **47** 511
[16] Kuch W, Lin M-T, Meinel K, Schneider C M, Noffke J and Kirschner J 1995 *Phys. Rev.* B **51** 12627
[17] Li C, Freeman A J and Fu C L 1988 *J. Magn. Magn. Mater.* **75** 53
[18] Luo H L and Duwez P 1963 *Can. J. Phys.* **41** 758
[19] Fassbender J, Allenspach R and Dürig U 1997 *Surf. Sci.* **383** L742
[20] Poulopoulos P, Jensen P J, Ney A, Lindner J and Baberschke K 2002 *Phys. Rev.* B **65** 064431